

Defect modes in one-dimensional photonic lattices

Francesco Fedele and Jianke Yang

Department of Mathematics and Statistics, University of Vermont, Burlington, Vermont 05401

Zhigang Chen

Department of Physics and Astronomy, San Francisco State University, San Francisco, California 94132

Received January 5, 2005

Linear defect modes in one-dimensional photonic lattices are studied theoretically. For negative (repulsive) defects, various localized defect modes are found. The strongest confinement of the defect modes appears when the lattice intensity at the defect site is nonzero rather than zero. When launched at small angles into such a defect site of the lattice, a Gaussian beam can be trapped and undergo snake oscillations under appropriate conditions. © 2005 Optical Society of America

OCIS codes: 190.5530, 230.3990.

Light propagation in periodic photonic lattices is under intensive study these days due to their novel physics and light-routing applications.^{1,2} Most of these studies focused on nonlinear light behavior in uniformly periodic lattices.^{3–10} A natural question arises: how does light propagate if the photonic lattice has a local defect? In photonic crystals, this question has been much analyzed.¹¹ While nonuniform arrays of fabricated waveguides with structured defects were used in previous studies,^{12–14} the issue of defect modes in optically induced photonic lattices has not yet received much attention. Since photonic lattices differ from photonic crystals in many aspects (for instance, the refractive-index variation in an induced photonic lattice is typically several orders of magnitude smaller than that in a photonic crystal), one wonders if photonic lattices with a local defect can also support defect modes.

In this Letter we theoretically analyze linear defect modes in one-dimensional photonic lattices with a local negative defect as induced in a biased photorefractive crystal. In such a defect the lattice intensity is lower than that at nearby sites (akin to air defects in photonic crystals¹¹), thus light has a tendency to escape from the defect to nearby sites. However, we found that localized defect modes exist as a result of repeated Bragg reflections. More interestingly, strongly confined defect modes appear when the lattice intensity at the defect site is nonzero rather than zero. As the lattice potential increases (by raising the bias field), defect modes move from lower bandgaps to higher ones. If a Gaussian beam is launched at small angles into the defect, it can be trapped and undergo robust snake oscillations inside the defect site without much radiation.

The physical situation that we consider here is that of an ordinarily polarized lattice beam with a single-site negative defect launched into a photorefractive crystal. This defected lattice beam is assumed to be uniform along the direction of propagation. Meanwhile, an extraordinarily polarized probe beam with a low intensity is launched into the defect site, propagating collinearly with the lattice beam. The nondi-

mensionalized model equation for the probe beam is⁵

$$iU_z + U_{xx} - \frac{E_0}{1 + I_L(x)}U = 0. \quad (1)$$

Here U is the slowly varying amplitude of the probe beam, z is the propagation distance (in units of $2k_1D^2/\pi^2$), x is the transverse distance (in units of D/π), E_0 is the applied DC field [in units of $\pi^2/(k_0^2n_e^4D^2r_{33})$], $I_L = I_0 \cos^2 x[1 + \epsilon f_D(x)]$ is the intensity function of the photorefractive lattice (normalized by the dark irradiance of the crystal, I_d), I_0 is the peak intensity of the otherwise uniform photonic lattice (i.e., far from the defect site), $f_D(x)$ is a localized function describing the shape of the defect, ϵ controls the strength of the defect, D is the lattice spacing, $k_0 = 2\pi/\lambda_0$ is the wave number (λ_0 is the wavelength), $k_1 = k_0n_e$, n_e is the unperturbed refractive index, and r_{33} is the electro-optic coefficient of the crystal. In this Letter we assume that the defect is restricted to a single lattice site at $x=0$. Thus, we take $f_D(x) = \exp(-x^8/128)$. Other choices of defect functions f_D give similar results. When $\epsilon < 0$, the light intensity I_L at the defect site is lower than that at the surrounding sites. This is called a negative (repulsive) defect where light tends to escape to nearby lattice sites. For $\epsilon = -1$ and -0.5 , the corresponding lattice intensity profiles are displayed in Figs. 1(a) and 3(b), respectively. In the former case there is no light at the defect site, while in the latter case there is still light at the defect site but with a halfway reduced intensity. These lattices with structured defects might be generated experimentally by optical induction. Consistent with our previous experiments,⁷ we choose the parameters as follows: lattice intensity $I_0 = 3I_d$, lattice spacing $D = 20 \mu\text{m}$, $\lambda_0 = 0.5 \mu\text{m}$, $n_e = 2.3$, and $r_{33} = 280 \text{ pm/V}$. One x unit corresponds to $6.4 \mu\text{m}$, one z unit corresponds to 2.3 mm , and one E_0 unit corresponds to 20 V/mm in physical units.

For a negative defect, a surprising feature is the possible existence of localized defect modes that are due to repeated Bragg reflections. We seek such

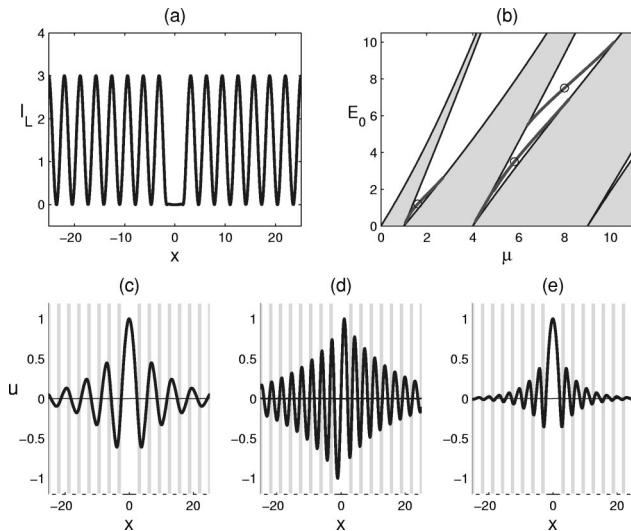


Fig. 1. (a) Lattice intensity profile with $I_0=3$ and $\epsilon=-1$. (b) Applied dc field parameter E_0 versus the defect eigenvalues μ ; the shaded regions are Bloch bands. (c)–(e) Three defect modes at $(E_0, \mu)=(1.2, 1.604)$, $(3.5, 5.812)$, $(7.5, 7.997)$, marked by circles in (b). The shaded stripes indicate the locations of the lattice's peak intensities.

modes in the form $U(x, z) = \exp(-i\mu z)u(x)$, where function $u(x)$ is localized in x and μ is a propagation constant. Our numerical method is to expand the solution $u(x)$ into discrete Fourier series, then convert the linear $u(x)$ equation into an eigenvalue problem with μ as the eigenvalue. First, we consider the defect with $\epsilon=-1$, where the lattice intensity at the defect is zero [see Fig. 1(a)]. For this defect, we have found defect modes at various values of E_0 . The results are shown in Fig. 1(b). It is seen that at low values of E_0 (low potential) two defect modes appear in the first and second bandgaps. The one in the first bandgap is symmetric in x , while the one in the second bandgap is antisymmetric in x . Both types of defect mode are moderately confined. Examples of such modes are displayed in Figs. 1(c) and 1(d), respectively. However, these defect modes disappear when E_0 increases above certain threshold values. In particular, the symmetric branch in the first bandgap disappears when $E_0 > 2.8$, while the antisymmetric branch in the second bandgap disappears when $E_0 > 7.5$. On the other hand, before the antisymmetric branch disappears, another symmetric branch of defect modes appears inside the same (second) bandgap. This new branch exists when $5.3 < E_0 < 10.3$, and it is generally more localized than the previous two branches. This can be seen in Fig. 1(e), obtained at $E_0=7.5$. Compared with the modes in Figs. 1(c) and 1(d), this new mode is much more confined.

Three general features in Fig. 1(b) should be noted. First, for any positive E_0 value, at least one defect mode can be found. Second, each branch of defect modes disappears as E_0 increases to above a certain threshold. In other words, defect modes move from lower bandgaps to higher ones as E_0 increases.

The existence of these defect modes as well as their profile and symmetry properties have a profound ef-

fect on linear light propagation in the underlying defected photonic lattices. If the input probe beam takes the profile of a defect mode, then it will propagate stationarily and not diffract at all. This is seen in Fig. 2(b), where the numerical evolution of an initial defect mode (with $\epsilon=-1$ and $E_0=7.5$) is displayed [the corresponding lattice field is shown in Fig. 2(a)]. This evolution was simulated using the pseudospectral method. For a Gaussian input beam (as is customary in experimental conditions), the evolution will critically depend on whether a defect mode resembling the input Gaussian beam exists under the same physical conditions. To demonstrate, we take an initial Gaussian beam as $U(x, 0) = \exp[-(1/3)x^2]$, which resembles the central hump of the defect mode in Fig. 1(e), and simulate its evolution under various E_0 values. The lattice intensity pattern is the same as that in Fig. 2(a) (where $\epsilon=-1$). We found that at small values of E_0 the Gaussian beam strongly diffracts and quickly becomes invisible. Similar behavior persists as E_0 increases [see Fig. 2(c)] until it reaches a value of ~ 7.5 , when a large portion of the initial beam's energy is trapped inside the defect site and propagates stationarily [see Fig. 2(d)]. As E_0 increases beyond 7.5, however, strong diffraction of the probe is seen again [see Fig. 2(e)]. These results indicate that the light trapping shown in Fig. 2(d) could not be attributed to either simple guidance resulting from increased lattice potential or nonlinear self-action of the probe beam itself. Rather, it must be attributed to repeated Bragg reflections inside the photonic lattice under certain phase-matching conditions, as the Gaussian beam matches the localized mode of the defect. This bears strong resemblance to localized modes in photonic crystal fibers.

In applications, it is often desirable to keep the defect modes as locally confined as possible. The defect considered above with $\epsilon=-1$ [see Figs. 1(a) and 2(a)] is certainly simple, but does it give the most strongly

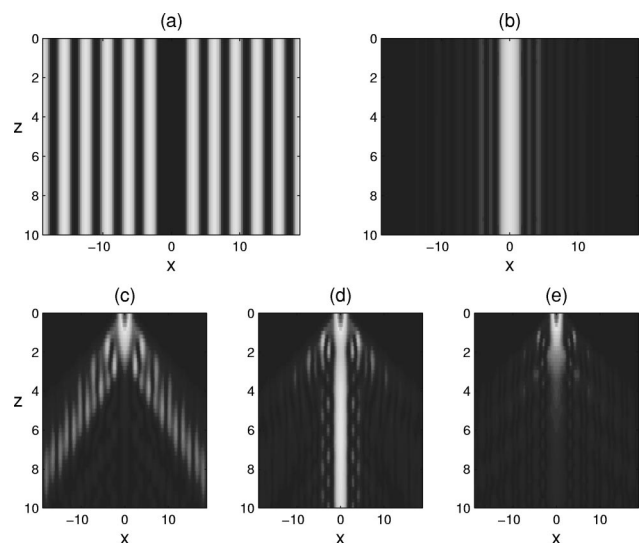


Fig. 2. (a) Lattice intensity pattern with $I_0=3$ and $\epsilon=-1$. (b) Evolution of an exact defect mode [shown in Fig. 1(e)] at $E_0=7.5$. (c)–(e) Evolutions of a Gaussian beam at E_0 values of 5, 7.5, and 10, respectively.

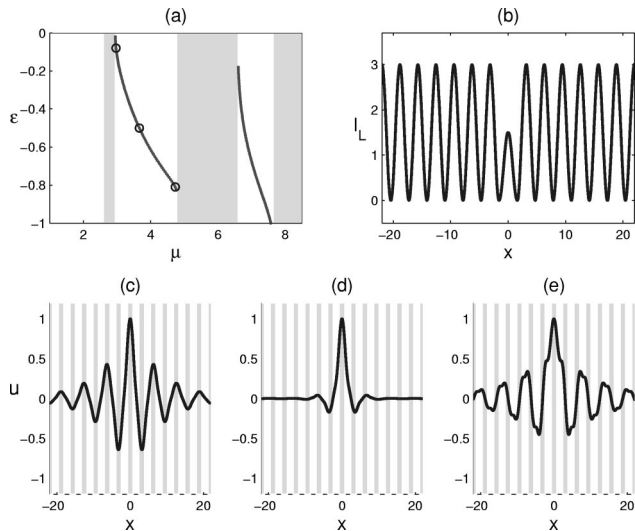


Fig. 3. (a) Defect strength ϵ versus the defect eigenvalues μ . (b) Intensity profile $I_L(x)$ of the photonic lattice with $\epsilon = -0.5$. (c)–(e) Three defect modes of the first bandgap with (ϵ, μ) , marked by circles in (a).

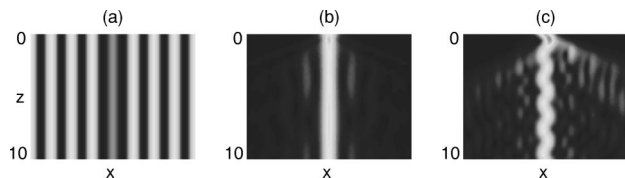


Fig. 4. Evolution of a Gaussian beam launched at zero (b) and nonzero (c) angles into the defect site of a photonic lattice shown in (a). Here $I_0=3$, $E_0=6$, and $\epsilon=-0.5$ in Eq. (1). The initial phase gradient in (c) is $k=1$.

confined defect modes? To answer this question, we fix the value of E_0 and allow the defect parameter ϵ to vary from -1 to 0 , then determine at what ϵ values the most localized defect modes arise. With fixed $E_0=6$, we obtain the defect modes versus ϵ and plot the results in Fig. 3. Figure 3(a) reveals that at small negative values of ϵ a single defect mode bifurcates from an edge of a Bloch band inside each bandgap. As ϵ decreases, the defect mode in the first bandgap disappears (at $\epsilon=-0.81$), while the one in the second bandgap persists. The defect-mode branch in the first bandgap is more localized than the one in the second bandgap in general. Thus we focus on this branch in the first bandgap below. When $|\epsilon|$ is small, the defect eigenvalue is rather close to the left Bloch band, thus the defect mode is rather weakly confined [see Fig. 3(c)]. As $|\epsilon|$ increases, the mode becomes more confined. As ϵ approaches -0.81 , the defect eigenvalue approaches the right Bloch band, and the defect mode becomes less confined again [see Fig. 3(e)]. Surprisingly, we found that the strongly confined defect mode occurs when $\epsilon \approx -0.5$. This defect mode and the corresponding lattice intensity field are shown in Figs. 3(d) and 3(b), respectively. These findings are rather interesting, as they show that the most localized defect mode arises when the lattice intensity at the defect site is nonzero rather than zero.

We further studied the evolution of a Gaussian input beam launched at small angles into a photonic lattice with $E_0=6$ and $\epsilon=-0.5$. For this purpose, we take the initial condition as $U(x,0)=\exp[-(1/2)x^2+ikx]$, where this Gaussian intensity profile resembles the central hump in the defect mode of Fig. 3(d), and the phase gradient k is proportional to the launch angle of the Gaussian beam. At zero launch angle ($k=0$), a vast majority of the input beam's energy is trapped inside the defect and propagates stationarily [see Fig. 4(b)]. Compared with Fig. 2, we see that the confinement of the probe beam by the present defect [shown in Fig. 4(a)] is more efficient, mainly because the defect mode admitted under these conditions is more localized [see Fig. 3(d)]. Next we take $k=1$, which corresponds to a launch angle of 0.58° with the physical parameters listed above. In this case most of the light is still trapped inside the defect site. However, the trapped light undergoes robust snakelike oscillations as it propagates through the defect [see Fig. 4(c)]. The ability of a negative defect to trap oscillating light beams is a remarkable feature that merits further investigation.

This work was supported in part by the U.S. Air Force Office of Scientific Research, NASA Experimental Program to Stimulate Competitive Research grants, and the Army Research Office. J. Yang's e-mail address is jjyang@math.uvm.edu.

References

1. D. N. Christodoulides, F. Lederer, and Y. Silberberg, *Nature* **424**, 817 (2003).
2. D. K. Campbell, S. Flach, and Y. S. Kivshar, *Phys. Today* **57**(1), 43 (2004).
3. A. B. Aceves, C. De Angelis, S. Trillo, and S. Wabnitz, *Opt. Lett.* **19**, 332 (1994).
4. H. S. Eisenberg, Y. Silberberg, R. Morandotti, A. R. Boyd, and J. S. Aitchison, *Phys. Rev. Lett.* **81**, 3383 (1998).
5. J. W. Fleischer, T. Carmon, M. Segev, N. K. Efremidis, and D. N. Christodoulides, *Phys. Rev. Lett.* **90**, 023902 (2003).
6. D. Neshev, E. Ostrovskaya, Y. Kivshar, and W. Krolikowski, *Opt. Lett.* **28**, 710 (2003).
7. H. Martin, E. D. Eugenieva, Z. Chen, and D. N. Christodoulides, *Phys. Rev. Lett.* **92**, 123902 (2004).
8. J. Yang, I. Makasyuk, A. Bezryadina, and Z. Chen, *Opt. Lett.* **29**, 1662 (2004).
9. R. Iwanow, R. Schiek, G. I. Stegeman, T. Pertsch, F. Lederer, Y. Min, and W. Sohler, *Phys. Rev. Lett.* **93**, 113902 (2004).
10. Y. V. Kartashov, V. A. Vysloukh, and L. Torner, *Phys. Rev. Lett.* **93**, 093904 (2004).
11. J. D. Joannopoulos, R. D. Meade, and J. N. Winn, *Photonic Crystals: Molding the Flow of Light* (Princeton U. Press, 1995).
12. U. Peschel, R. Morandotti, J. S. Aitchison, H. S. Eisenberg, and Y. Silberberg, *Appl. Phys. Lett.* **75**, 1348 (1999).
13. A. A. Sukhorukov and Yu. S. Kivshar, *Phys. Rev. Lett.* **87**, 083901 (2001).
14. R. Morandotti, H. S. Eisenberg, D. Dandelik, Y. Silberberg, D. Modotto, M. Sorel, C. R. Stanley, and J. S. Aitchison, *Opt. Lett.* **28**, 834 (2003).